Controlling Drop Coalescence Using Nano-Engineered Surfaces

by

Manuel Corral Jr.

Submitted to the Department of Mechanical Engineering
in partial fulfillment of the requirements for the degree of

Bachelors of Science in Engineering as Recommended by the
Department of Mechanical Engineering

at the

MASSACHUSETTS INSTITUTE OF TECHNOLOGY

June 2011

Signature of Author.....
Department of Mechanical Engineering
May 11, 2011

Certified by.....
Kripa K. Varanasi
Assistant Professor
Thesis Supervisor

Accepted by.....
John H. Lienhard V
Samuel C. Collins Professor of Mechanical Engineering
Chairman, Undergraduate Thesis Committee

Controlling Drop Coalescence Using Nano-Engineered Surfaces

by

Manuel Corral Jr.

Submitted to the Department of Mechanical Engineering
on May 11, 2011, in Partial Fulfillment of the
Requirements for the Degree of
Bachelors of Science in Engineering as Recommended by the
Department of Mechanical Engineering

ABSTRACT

The dynamics of drop coalescence are explored on micro-scale surface features for the first time. Drop coalescence is defined as a process by which two or more droplets, bubbles or particles merge during contact to form a single droplet, bubble or particle. There are two regimes that limit the dynamics of drop coalescence of a liquid. The first is regime is limited by the viscosity of the droplets. The second regime is limited by inertial forces caused by the motion that merges the two droplets. Currently, much work has been done to study drop coalescence in a liquid-liquid environment and the phenomenon has been well defined and modeled. Previous work has been done to understand liquid-liquid drop coalescence using liquids with varying viscosity, but the effects of solid micro-textured surfaces on drop coalescence dynamics of low density liquids, such as water, have not yet been analyzed and quantified. Very little has been studied about drop coalescence in a solid-liquid-air interface. In this thesis, drop coalescence in its inertial regime will be defined in low viscosity liquid, water, on surfaces with varying wettability and micro-scale features. Surfaces include microstructures consisting of a regular array of square posts defined by the aspect ratio of the posts and the spacing between the posts. This work focuses on the development of a fundamental understanding and physical model of micro-scale surface texture effects on drop coalescence to provide aid in future surface design applications. These applications could allow for the controlling of this phenomenon to promote drop-wise condensation in order to increase efficiencies of condensers or to aid in water-oil separation procedures.

Thesis Supervisor: Kripa K. Varanasi
Title: Assistant Professor

ACKNOWLEDGEMENTS

First and foremost, I would like to express my gratitude for the enthusiasm and dedicated guidance of my thesis advisor, Professor Kripa Varanasi. His energy and dedication to the progression of nano-engineering technology has inspired me tremendously and I have truly appreciated the opportunity to work on this project. Without his advice, I would not have been able to complete this thesis project.

I would also like to thank Katherine Smyth for her guidance throughout my project. Her consultation and constant words of encouragement have allowed me to complete a project that I believe to be valuable for future works in the Varanasi Group. All the members of the Varanasi Group have also been of great assistance, offering advice whenever possible. I am truly grateful for having had the opportunity to be a part of the Varanasi Group the past year and a half.

I would also like to express appreciation for my academic advisor, Professor Alexander Slocum for his advice and support during my time at MIT. His encouragement has been a major motivation for me, inspiring me to constantly push myself further than I thought possible.

As I move on from MIT, I will not forget the support I have and will continue to receive from my parents, Norma and Manuel Corral, and my siblings, Celina, Natalie, and Nicholas, for their tremendous love and encouragement. Their support not only aided in my eventual arrival to MIT, but through it as well, and I could not be more grateful.

Contents

List of Figures

1 Introduction

1.1 History and Motivation

The exploration of drop coalescence dynamics is largely motivated by its importance for a number of technological processes and its key role in drop nucleation and condensation. With applications in power and water desalination plants, previous works have focused on surface wetting properties that would enhance the heat transfer across a given surface. Condensation on surfaces can often create thin liquid films over a surface resulting in decreased heat transfer and decreased plant efficiency. However, when vapor condenses in the form of droplets on a surface, the heat transfer and efficiency increase greatly. Initial exploration of drop coalescence has helped define critical conditions that largely affect the dynamics of low viscosity drops during spreading and coalescence [1]. The understanding of these conditions will ultimately allow for the optimization of surfaces for increased heat transfer across a surface.

The foundation for many of these discoveries root from surface wetting studies performed as a means of defining the contact angle of a liquid on a surface based on surface free energies in the system. Surface wetting studies have been able to characterize wetting on rough or heterogeneous surfaces through modification of the contact angle equation developed by Young [11,12].

Due to its rapid nature, previous studies have found it difficult to observe the coalescence phenomena or develop experiments to reliably provide accurate data on the process [1]. More recent studies have been able to examine water using methods that slow the approach velocities enough reliably obtain data. This work has provided a detailed study of the viscous to inertial crossover dynamics for liquid drop coalescence [4]. The ability to predict and essentially "control" drop coalescence to favor dropwise condensation would benefit geothermal, water desalination and nuclear plants by minimizing the formation of films on tank surfaces. With less formation of liquid films,

heat transfer is maximized and there is a significant decrease in losses resulting in much higher plant efficiencies.

1.2 Fundamentals of Drop Coalescence

Vast amounts of research have been done to understand the stand alone phenomenon of drop coalescence. The physical model of drop coalescence has been developed analytically and has been confirmed experimentally. The process begins when two droplets approach each other at negligible velocities and van de Waals force join the two drops together to form a tiny liquid bridge [5]. After the bridge formation, two regimes limit the kinetics of drop coalescence to its completion. The entire process from bridge formation to complete coalescence has been experimentally determined to last between 10μs to 200μs, depending on the size of the droplets [6]. Initially, there is a viscous regime in which the motion of the droplets is limited by the viscosity of that particular liquid. Almost immediately after the process begins, roughly 2μs after initial contact, an inertial regime becomes the limiting factor due to an increase in velocity of the two droplets merging together [4]. This crossover behavior is attributed to the dimensionless Reynolds number that relates both viscous and inertial forces. The Reynolds number is often used to quantify the importance of the two types of forces for given flow conditions. The two variables affecting the Reynolds number for a given liquid are the characteristic velocity, V, and length, L, as shown in equation 1.1.

$$Re = \frac{\rho V L}{\mu} \qquad [1.1]$$

Equation 1.1 shows the Reynolds number as a function of the characteristic parameters, density, ρ, and viscosity, μ. Experimentally, it has been shown that the coalescence dynamics of droplets is driven by surface tension, and slowed down by viscosity for low and by inertia for high Reynolds numbers [3]. The crossover between the two regimes is

expected at Re ≈ 1, where the viscous forces are relatively equal to the inertial forces acting on the process [4].

$$\text{Re} < 1 : \text{Viscous forces dominate}$$
$$\text{Re} > 1 : \text{Inertial forces dominate}$$

At the initial contact of two water droplets, a singularity occurs due to the inversion of one of its two radii of curvature. The water droplets connect and a liquid bridge forms between the droplets. This bridge radius grows linearly with time throughout the viscous regime of drop coalescence, but grows at a rate proportional to $\sqrt{t}$ during the inertial regime [3]. Figure 1-1 shows a top view of the bridge progression during drop coalescence.

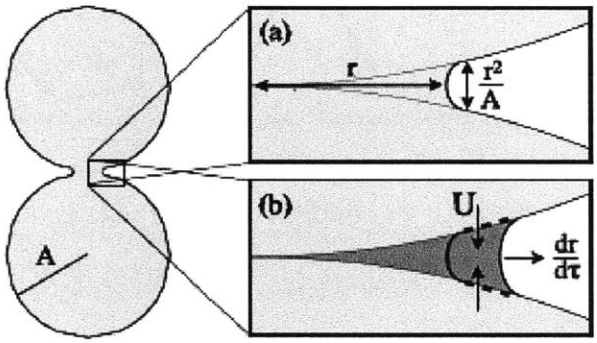

Figure 1-1: (a) Bridge formation at start of inertial regime (b) expansion of the bridge in the radial direction. The speed of the flow will be defined as $V = \frac{1}{2} * \frac{dr}{dt}$ [4]

Viscous Regime

The viscous regime of drop coalescence, known for lasting only for a small fraction of the total time it takes for two drops to coalesce (~2μm), plays a key role in initiating the dynamics of the process and has been studied to some extent in the past [2,6]. Upon initial bridge formation between the two drops, the opening velocity of the bridge results from a competition between the capillary forces that drive the coalescence, and the viscous forces that attempt to slow it down. During this regime, it can be expected from recently established viscous dynamics that the capillary velocity scales as:

$$V = \gamma/\mu \qquad [1.2]$$

Where γ is the surface tension and μ is the viscosity [3]. One study experimentally quantified the width rate of change for the neck that bridges a drop and bulk fluid during coalescence [7]. The interface for the study was a liquid-liquid-liquid interface in a Hele-Shaw cell, but the dynamics of the neck that bridged the two fluids matched predicted data for the width change of rate for prior studies. The bridge, shown in Figure 1-2, was used to determine the crossover between the two regimes.

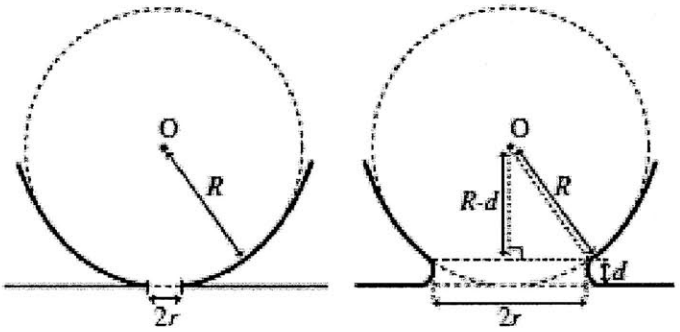

Figure 1-2: Geometry of the neck that bridges the two fluids involved in coalescence at short-time (left) and long-time (right). Defined parameters are the neck width 2r, neck length d, and radius diameter R [7].

Inertial Regime

Upon crossover into the inertial regime, the motion of the droplets being driven by surface tension is then limited by the inertia of the fluids coalescing. For liquids with low viscosity, such as water, the widening of the neck that bridges the two fluids is opposed primarily by inertial forces instead of viscous forces [8]. It is due to this fact that coalescence is in the inertial regime for almost the entire process, up from two decades longer than the viscous regime. As the bridge continues to grow between the two droplets, capillary waves begin propagating outward from the bridge. In systems where a drop coalesces with a bulk fluid, a time scale is associated with the surface-tension driven distortions of a drop that depend on the surface tension σ, drop size D, and its density ρ, shown in equation 1.3 [14].

$$\tau_\sigma = \sqrt{\frac{\rho * D^3}{\sigma}} \qquad [1.3]$$

1.3 Wettability of micro- and nano-textured surfaces

Young's Relation

When a liquid is deposited onto a solid in a vapor environment, as shown in figure 1-3, there is a balance of surface tensions acting at the solid-liquid-vapor contact line, the border created by the drop on the substrate where the three phases of the system exist. This balance of surface tensions at the interface of the three phases is characterized by the Young equation for contact angle. This equation, also used to characterize surface energies with displacement, dx, (shown in figure 1-4) of the contact line, describes the phenomena of each phase impacting the contact line to minimize the corresponding surface area [10].

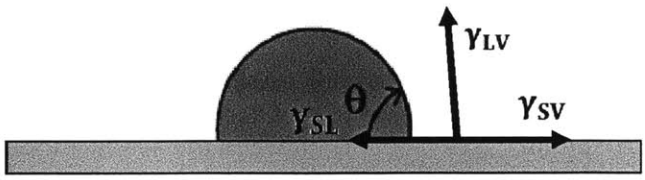

Figure 1-3: A drop on a solid in a vapor environment with contact angle θ. The arrows denote the direction of each surface tension, γ, where LV is liquid-vapor, SV is solid-vapor, and SL is solid-liquid. Young's equation describes the relationship between the three.

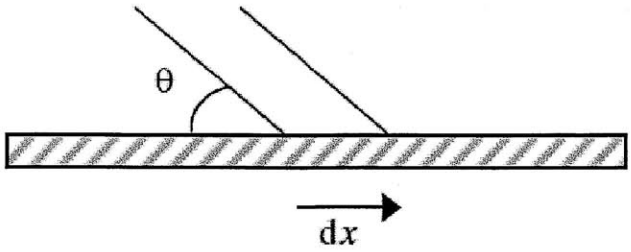

Figure 1-4: Displacement of the contact line by distance, dx, modifies the surface area of each interface affecting the Young equation

The Young equation for contact angle with respect to the three surface tensions is shown in equation 1.4 and is used to determine the equation representing the change of energy with respect to all surface tensions, shown in equation 1.5.

$$cos(\theta) = \frac{\gamma_{SV} - \gamma_{SL}}{\gamma_{LV}} \quad [1.4]$$

$$dE = \{(\gamma_{SL} - \gamma_{SV}) + \gamma_{LV} * \cos(\theta)\} * dx \quad [1.5]$$

The Young model, however, only considers the ideal case where the solid surface is smooth and free of heterogeneities. Young's fundamental model has been corrected in order to take into consideration the roughness of a surface. Robert Wenzel was able to modify the Young equation to take the surface roughness into account when solving for the surface tensions at the three phase contact line. Wenzel defined the roughness factor, shown in equation 1.6, to make a distinction between the actual surface and the geometric surface, the surface as measured in the plane of the interface [11].

$$r = \frac{actual\ surface}{geometric\ surface} \quad [1.6]$$

The roughness factor is then multiplied by the adhesion tension between the liquid and the solid to account for the influence of the surface on the observed contact angle, θ', as shown in equation 1.7.

$$cos(\theta') = \frac{r(\gamma_{SV} - \gamma_{SL})}{\gamma_{LV}} = r * \cos(\theta) \quad [1.7]$$

Cassie and Baxter developed a model that is used to account for the influence of a heterogeneous surface, a case where the Wenzel model is not sufficient [12]. This model yields a definition for the apparent contact angle on a composite surface shown in equation 1.8.

$$\cos(\theta'') = f_1 * \cos(\theta_1) + f_2 * \cos(\theta_2) \quad [1.8]$$

Where θ'' is the contact angle on the composite surface, f is the fraction of the solid surface area wet by each component, and θ is the contact angle for each component on the composite surface.

In the Cassie-Baxter model, a droplet sits on a textured surface where air is trapped underneath. As the air pockets lose thermodynamic stability, a wetting transition occurs and liquid begins to fill the air pockets until the surface energy is minimized, at which point it is in the Wenzel state, shown in figure 1-5.

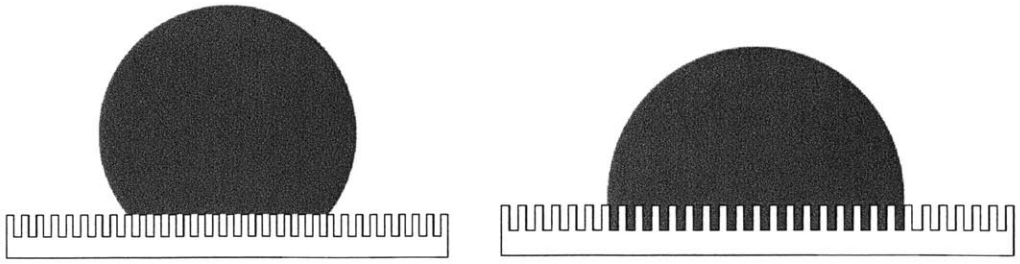

Figure 1-5: Cassie-Baxter model (left) and the Wenzel model (right) after having gone complete wetting transition

The wettability of a surface is a key parameter that aids in the characterization of a surface. Significant work has been done with surface design to obtain a desired wettability with micro- and nano-features present on a surface.

Hydrophobic Surfaces

Many developments in creating hydrophobic surfaces have been made in recent years due to many of the advantages a surface can gain by increasing its hydrophobicity. Much work began when naturally occurring superhydrophobic surfaces, with contact angles upward of 155°, were recognized as having excellent roll-off and self-cleaning properties [15]. One example of such a naturally occurring surface is the Lotus Leaf. The Lotus Leaf, shown in figure 1-7, has a network of nanostructures branching from a network of microstructures that easily allow rain drops to roll or bounce off the leaves, picking up dirt, particles and dust along the way. Wax crystals compose the nanostructure on the microstructured epidermal cells of the plant.

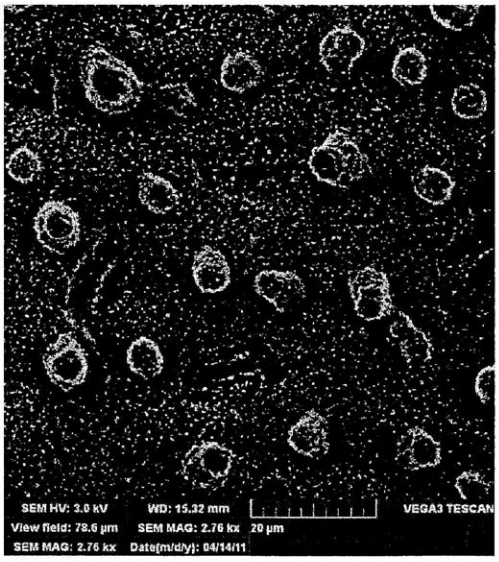

Figure 1-7: SEM Image of Lotus Leave at 2.76k magnification

More relevant to the application of this thesis, emphasis will be placed on photo lithographically fabricated square microposts on a silicon wafer. Previous work to design micropost surfaces has determined that the wetting state of a sessile drop greatly impacts the roll-off behavior of that drop [16]. An optimal wetting region was determined to have

the lowest roll-off angles contrary to the initial expectation that Cassie state droplets would yield the lowest roll-off angles. It is important to note that the hydrophobicity of a surface does not directly correlate with the associated hysteresis of that surface.

Contact Angle Hysteresis

Many parameters help characterize the wetting of a droplet on a surface. Two key parameters include the advancing, θ_{adv}, and receding, θ_{rec}, contact angles of a droplet on a surface. The difference between the two contact angles yields a parameter called contact angle hysteresis, $\Delta\theta$, as shown in equation 1.9.

$$\Delta\theta = \theta_{adv} - \theta_{rec} \qquad [1.9]$$

The hysteresis exhibited for a particular fluid on a surface is caused by a pinning of the fluid to the surface at the three phase contact line. Recent works have re-surfaced the exploration of hysteresis for the increasing interest in superhydrophobic and self-cleaning surfaces. In order to observe hysteresis, a droplet on a surface must either advance or recede along the entire three phase contact line by way of increasing the liquid-vapor interfacial area and energy to move the droplet as shown in figure 1-6 [19]. Experiments done to cause this movement involve tilting the surface on which the drop sits until roll-off occurs.

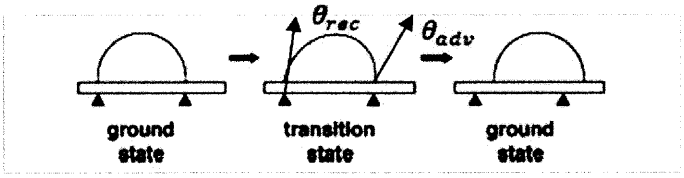

Figure 1-6: Advancing and receding angle during transition state caused by movement of the droplet.

Aside from roll-off methods of solving for hysteresis, volume addition is also used to identify the advancing and receding contact angles. Volume is added until an advancing angle is observed and is then removed until a receding angle is observed.

Generally, when high hysteresis is observed, there is a strong resistance to motion of the droplet. Development of a pinning parameter has helped describe the hysteresis of a droplet on a textured surface to determine roll-off properties associated with that particular surface [16].

1.4 Drop Impact Dynamics

When a liquid drop impacts a solid, it spreads out across the surface up to the point where all the kinetic energy is dissipated by viscosity. Then, depending on how hydrophobic the surface is, the droplet can retract. On surfaces where such phenomenon is observed, the kinetic energy of the impinging drop can be transferred to surface energy, without spreading. In this case, the drop can fully bounce. The restitution coefficient is solved for in order to characterize a liquid's "elasticity" during a bounce.

$$\varepsilon = V'/V \qquad [1.10]$$

Where V and V' are, respectively, the velocities before and after the impact measured for each bounce. The dimensionless number that compares the kinetic energy to the surface energy is the Weber number. This expression describes the droplet behavior based on the droplet size and the droplet height.

$$We = \frac{\rho V^2 R}{\gamma} \qquad [1.11]$$

Where γ is the liquid surface tension and ρ is its density.

When a droplet hits a surface, some of the kinetic energy is then stored in surface energy. In situation where the droplet is small enough such that the surface energy of the sphere is larger than the kinetic energy it gains during a drop, we are involved in a regime where the We << 1. Physically, this is representative of only a slight deformation of the liquid at contact with the surface. The deformation of the droplet upon colliding with the

surface is a spreading effect that turns the sphere into a disk (shown in figure 1-8). At this point, the droplet can retract to its original form or remain in a deformed state depending on the wettability of a surface. Surfaces with very little wetting would allow the droplet to return almost fully to its original shape.

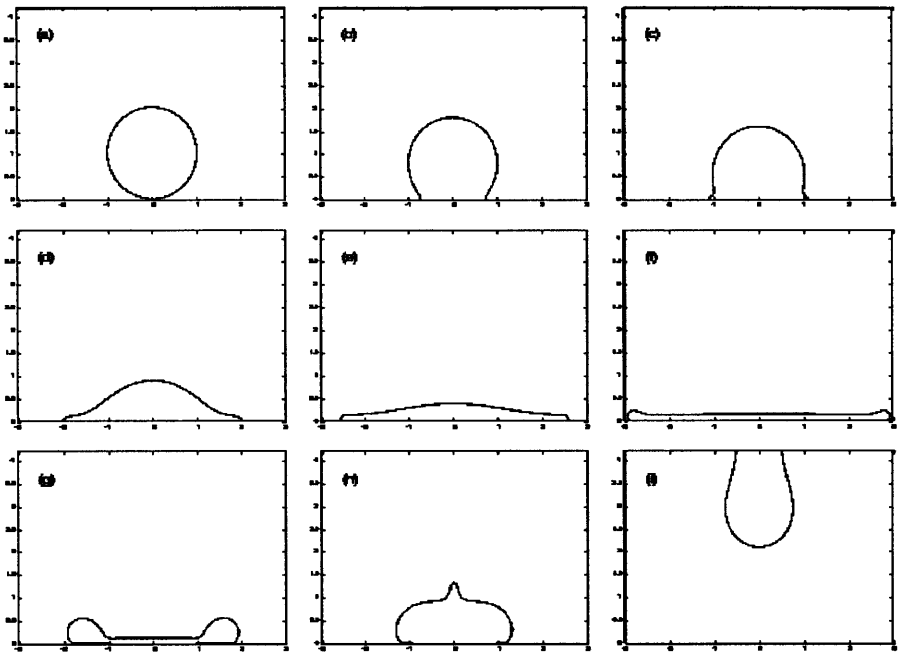

Figure 1-8: The top left image is of a water droplet at initial contact. The droplet then hits the surface and spreads as it dissipates its kinetic energy. The droplet then recoils, shown on the bottom left and proceeds to bounce back off the surface. [13]

The Reynolds number, as previously defined in equation 1.1, is also used to describe the dynamics of a droplet impacting surface. With a large Reynolds number, the inertial forces have a much greater effect than the viscous forces, thus limiting the viscous effects to the very thin boundary layer across the surface.

The flow patterns exhibited during drop impact on a dry surface can range greatly depending on the surface texture. Parameters such as wettability and roughness become important in the way the droplet forms when it impacts the surface. Different types of flow pattern include deposition, prompt splash, corona splash, receding break-up, partial

rebound and complete rebound [17]. For the purpose of this thesis, the receding break-up pattern will be observed (see figure 1-9).

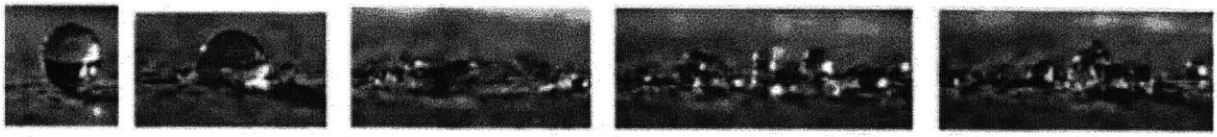

Figure 1-9: Morphology of Receding Break-Up Drop Impact on a Dry Surface [17]

When investigating surface with nonwettable properties, with contact angles approaching 180°, the thin water layer that forms upon impact, known as the lamella, shrinks and breaks off smaller fingers that can also break up further again due to capillary instability. At the end of the spreading stage, the surface and kinetic energy in the lamella can still be large enough that the drop can recede and have enough velocity to collapse and squeeze liquid up off the surface. Parameters that largely impact the scenario include velocity, surface tension, fluid viscosity, and receding contact angle, θ_{rec}.

Previous work has been done to empirically determine the correlation of the deposition-splashing boundary in terms of the Reynolds number and the Ohnesorge number [18]. The Ohnesorge number, a dimensionless parameter that relates viscous forces to inertial and surface tension forces is shown in equation 1.12. Large Ohnesorge numbers are indicative of a greater influence of the fluid viscosity where μ is the liquid viscosity, ρ is the liquid density, σ is the surface tension, and L is the characteristic length scale (typically the drop diameter).

$$Oh = \frac{\sqrt{We}}{Re} = \frac{\mu}{\sqrt{\rho * \sigma * L}} \qquad [1.12]$$

The determined correlation of the deposition-splashing boundary, K, could be explained through the aforementioned Oh and Re numbers shown in equation 1.13.

$$K = Oh * Re^{1.25} \qquad [1.13]$$

Where the critical K value, 57.7, for the splashing threshold during drop impact on a surface was empirically determined to yield the following relation:

$$K > 57.7 : \text{Incipient Splashing}$$
$$K < 57.7 : \text{Complete Deposition}$$

For this thesis, values of K are expected to exceed the threshold which yields incipient splashing during drop impact.

1.5 Objectives

The goal of this thesis is to define the inertial coalescence regime in low viscosity fluid, water, on surfaces with varying wettability and micro- and nano-scale features. The effects of micro- and nano-textured surfaces on drop coalescence dynamics will be investigated analytically and observed experimentally. The time dependent change in width of the two combined drops throughout the coalescence process will be measured to analyze the effects of surface structure on the droplet coalescence.

Initial exploration of drop coalescence defined critical conditions that largely affected the dynamics of low viscosity drops during spreading and coalescence. However, experimental findings using a solid-liquid-air interface in the past have not been able to yield reliable results due to strong oscillations of the water droplets induced by syringe deposition [1]. The oscillations induced by dropping water onto an already existing drop forced a "pulling" of the drops contact line which accelerated its motion and added too much energy into the low viscosity system. Other works have focused on the dynamics of high viscosity fluids to allow for a slowing down of the drop coalescence dynamics for proper observation. Low viscosity liquids have a rapid motion and, until recently, have made it difficult to carefully observe. Experimental results of the high viscosity drop coalescence agreed quite well with numerical simulations of the Stokes equations and provide a solid, fundamental understanding of the dynamics of two droplets during coalescence [2].

Two main techniques will be used to measure the effects of surface structure on drop coalescence. Slow volume addition will be used to bring two water droplets together close enough to induce coalescence. The width of the two drops from start to finish will then be measured using high speed video (10,000 fps) to experimentally determine the rate at which the width changes with respect to time during drop coalescence. Drop coalescence will further be explored by observing instantaneous drop impact of two low viscosity fluids at close proximity as to allow for coalescence of the two droplets. Satellite droplets that break from the merged liquid will be evaluated to determine the effects of surface structure on the drop coalescence during impact. High speed video of the vertical distance of the satellite droplets as well as the merged droplet will be used to experimentally determine the energy distribution of the system. A preliminary physical model of drop coalescence on surfaces with varying wettability and micro-scale features will be proposed to account for the difference in dynamics as a result of surface effects on the droplets.

It is the goal of this thesis to clearly define and develop a fundamental understanding of drop coalescence under the influence of varying surfaces for the development of surface design applications that would essentially allow for the control of the phenomenon to obtain desired results. This understanding will also open doors for a continuation of research in characterizing nano-engineered surfaces for implementation in commercial applications.

2 Experimental Procedure

2.1 Sample Preparation

Micro-post samples were prepared using four inch p-type wafers from Wafernet, Inc. The wafers were processed using standard photolithography for patterns of 10μm by 10μm posts with varying post spacing using Shipley 1813 as the photoresist. The photoresist was spin coated onto the wafer at 4000 rpm for 40 seconds to create an approximately 1.3μm thick layer. Three dimensional post geometries were etched into the surface using CF_4 plasma RIE achieving an etch depth of 10μm into the silicon substrate. The remaining photoresist was stripped and the surface was cleaned using a piranha solution (5:1 mixture of 98% H_2SO_4 and 30% H_2O_2) at 120°C creating micro-post arrays with 10μm post height. After cleaning, the substrates were placed in a vacuum dessicator in -25inHg relative pressure with two drops of trichloro(1H,1H,2H,2H-perfluorooctyl)silane (fluorosilane) for three hours forming a thin layer of fluorosilane on the substrate surface. Fluorosilane was deposited via vapor phase deposition onto the substrates to make the surface hydrophobic. The microstructure on each substrate is shown in Figure 2-1. When characterizing the surfaces, the surfaces will be defined by the aspect ratio of the post width, a, and the post spacing, b.

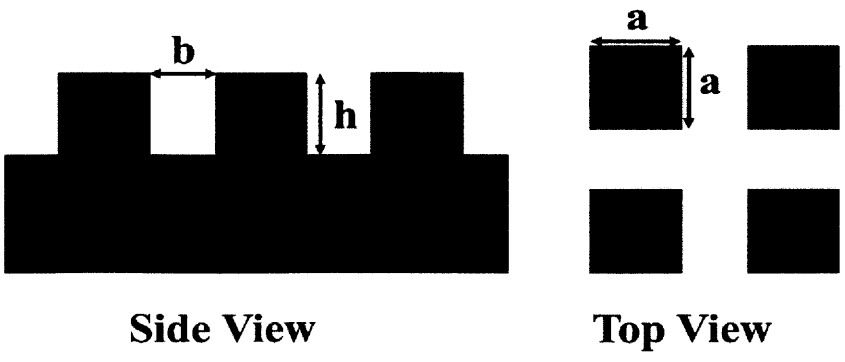

Figure 2-1: Profiles for samples used in experiment

2.2 Water Deposition Procedure

Measurements for the volume addition method were taken using a ramé-hart Model 500 Advanced Goniometer to provide the stage on which the experiments were performed. A ramé-hart automated dispensing system was used to deposit and add volume to water droplets on the substrates to induce the measured coalescence. In order to reduce the effect of ambient vibration in the system, the goniometer was placed on a Newport CM-225 Ultra-clean vibration damping system with four isolators.

The automated dispensing system allowed for continuous volume addition on a microliter scale. A 250μl syringe held the reservoir of deionized water used to conduct all experiments and was refilled every time the system indicated that water levels were low. The volume of water and the rate at which the volume of water was added was controlled using the Drop Volume Control interface using volume step and full stroke time settings. The full stroke time setting refers to the amount of time necessary to fully dispense the syringe volume. To derive the rate at which the volume is added, simply divide the volume of the syringe by the full stroke time. Since the full stroke time is inverse of the flow rate, higher stroke times would imply slower volume addition rates. For the purposes of this paper, it is essential that an extremely slow input rate is achieved because the relatively large oscillations that occur at fast volume addition rates can add unwanted energy to the system.

The surfaces on which the experiments were performed were micro-structured and smooth silicon substrates coated with a monolayer of fluorosilane. The micro-structured surfaces were patterned with 10μm by 10μm by 10μm square micro-posts with 3.3, 5, 7.5, 10, 15, 20, 25, 30, 40, 50, 75, 100 μm spacing in between posts. Drop condensation was measured on each substrate using the measurement technique specified in Appendix Section

2.3 High Speed Video

High speed video of drop coalescence on the substrates was taken using a Photron Fastcam SA1.1 High Speed Video camera. The lens used to image the droplets was the Nikon AF-S VR Micro-NIKKOR 105mm f/2.8G IF-ED lens designed for extreme close-up imaging. The Nikon AF-S Teleconverter TC-17E-II was also used in combination with the micro lens to enhance light transmission efficiency and to get a 1.7x optical conversion factor. Lighting was set-up behind the substrate to provide a stark contrast between the droplets on the substrate and the air surrounding the substrate and water droplets. In order to obtain the measurements, the camera was placed on a tripod and oriented facing the two droplets and the substrate parallel to the surface of the substrate. The entire experimental setup is shown in Figure 2-2.

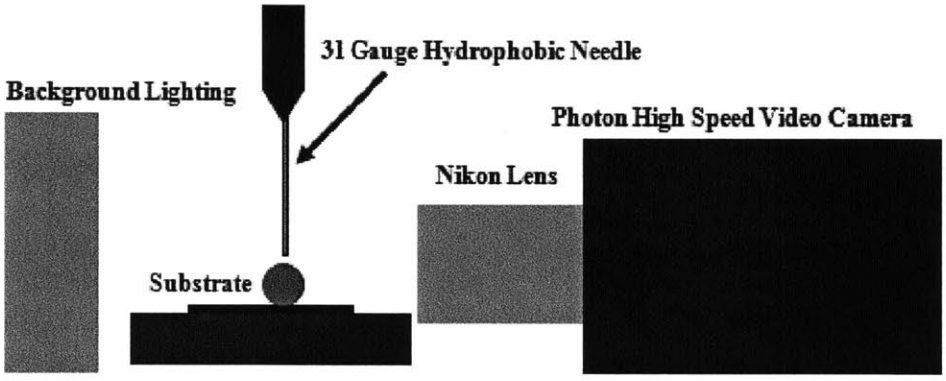

Figure 2-2: Setup for water deposition experiments.

Droplets were deposited onto the substrate that sat on the goniometer stage using the dispensing system described earlier. Initially, a drop was deposited on the substrate at a 600s stroke time. The lens was then focused on the droplet for optimum resolution of the droplet. After that, the syringe was moved directly next to the initial drop and the experiment was ready to be initiated. During the experiment, the high speed video camera, controlled by the Photron Fastcam Viewer software, imaged the coalescence process at 10,000 frames per second (fps) with a resolution of 1024x1024. The background light was modified to provide the optimum brightness and contrast. Figure

2-3 shows the actual set-up for volume addition experimentation. In order to level the camera, levels on the camera tripod indicated the exact orientation of the camera with respect to the ground.

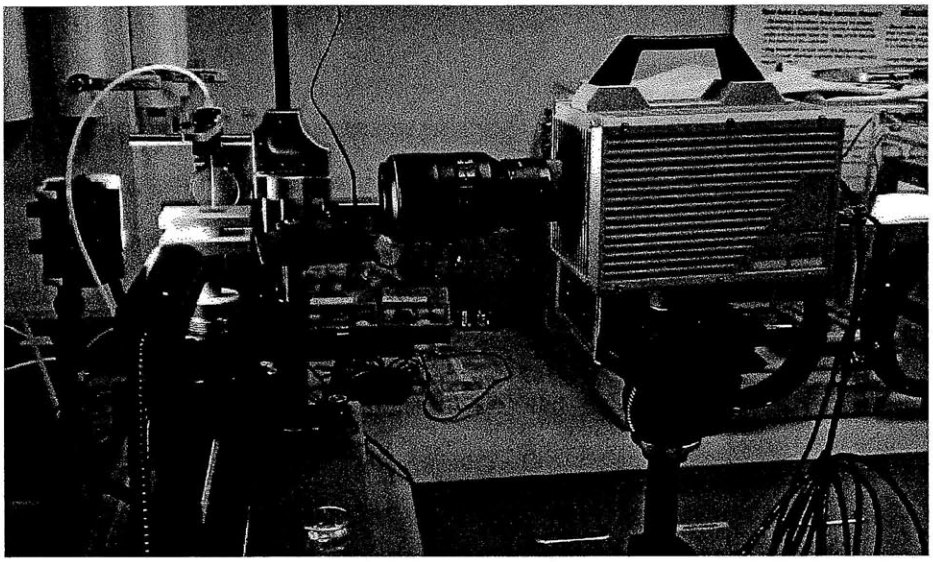

Figure 2-3: Experimental set-up for volume addition experimentation.

2.4 Design and Fabrication of Droplet Device

A key parameter for drop impact experimentation was that the drops land on the surface at the same time. In order to assure that both drops impacted the surface at the same time, a device was designed to release both drops instantaneously. The device needed to release the drops smoothly such that the drops maintained their spherical shape and oscillations in the drop on the way to the surface were kept to a minimum. The device, shown in figure 2-4, was designed with a 2cm wide drop plank that could hold a superhydrophobic surface with very low hysteresis. The surface allowed the drops to simply roll off when the plank was dropped. The mechanism that released the plank was a plunger that allowed the plank to rotate about a ¼" diameter rod using bushings to reduce the friction and play in the plank movement. The device itself could attach to a ½" rod that was connected to a laboratory stand using notched holes for tightening.

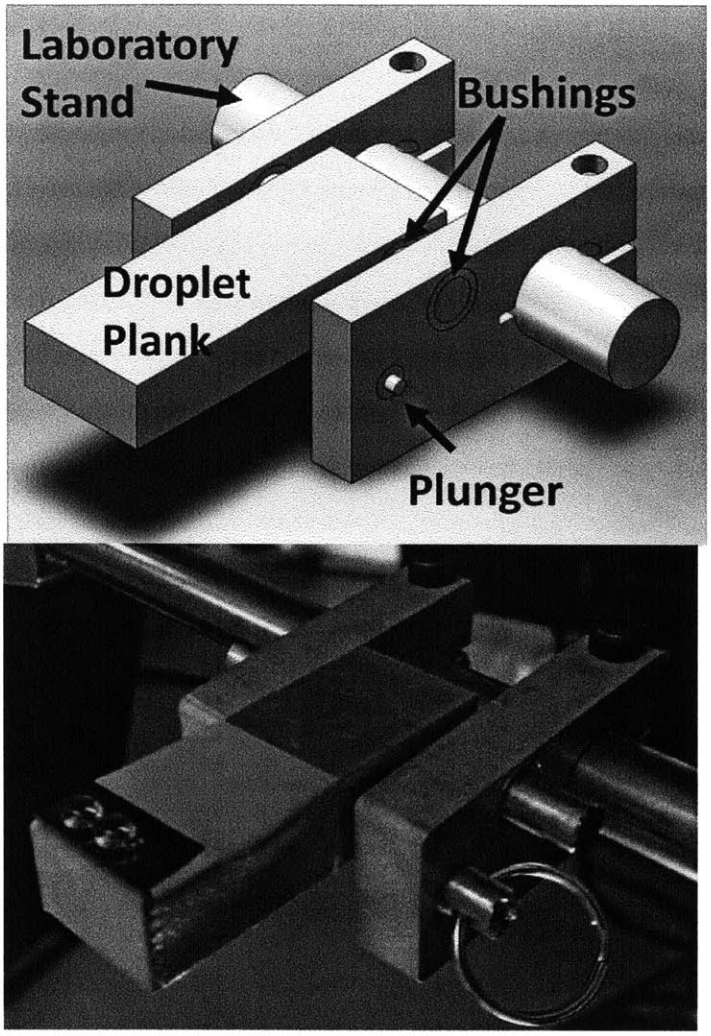

Figure 2-4: Design for droplet device.

Due to the setup for these particular experiments, the goniometer stage and droplet generator could not be used to place the drops on the surface. Instead, precision pipettes were used to place water droplets on the plank for testing. In order to ensure that the droplets remained spherical during the drop, droplets with small volume were used such that the surface tension of the water kept the drop from deforming drastically during the release of the plank.

When performing the experiments, a height of 30cm was chosen to ensure that the velocity was great enough to cause splashing of the droplets upon contact with the surface. The actual experimental set up was similar to the volume addition set up, but

instead of a needle gently adding liquid to the surface, the droplet device was attached to a laboratory stand at the desired height.

3 Modeling Drop Coalescence on a Microstructured Surface

3.1 Microstructure Impact on Drop Coalescence Rate

In addition to surface tensions acting at the three-phase boundary of the contact line formed by a sessile drop on a solid substrate, an additional force is added to the system when a drop coalesces with another drop right next to it, as shown in figure 3-1. As the drops coalesce, forces pull the drops toward each other until equilibrium is reached. The drop coalescence process behaves as a third order system where the large drop, comprised of the two smaller drops, oscillates about its equilibrium point until it dampens to a steady equilibrium position on the surface. The force caused by the two drops pulling together eventually gets eliminated and leaves the natural response of water and the solid-liquid interface to dampen the system to equilibrium. Since the experimental fluid, DI water, is the same across all the experiments, the interactions between the molecules of the fluid will remain fairly constant. However, the interaction between the solid and the liquid can vary quite drastically across a range of surfaces. This variance can be used to distinguish the effects of a microtextured surface on the dynamics of drop coalescence on its surface.

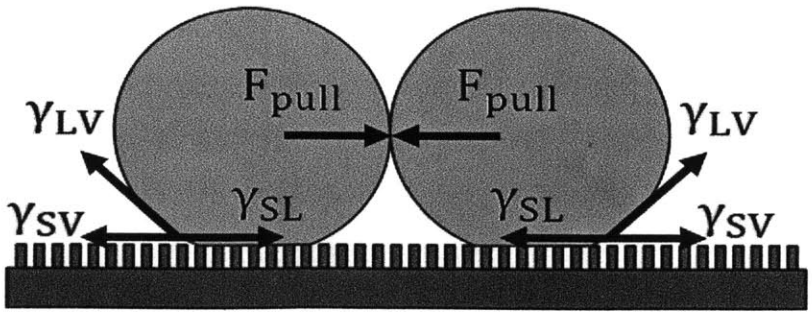

Figure 3-1: Force balance at initial contact of the two drops during coalescence.

Industrially, this information would be useful in applications involving condensers. A large resistance to movement on the surface would make the liquid more likely to form a film over the surface. In cases where it is necessary that there is heat transfer through the surface, films would be detrimental because they would significantly lower the efficiency of that particular heat exchanger. Smaller resistance to movement on the surface would indicate just the opposite. Rather than film formation at the surface, drop formation would be the more likely to occur; a result which would increase the heat transfer and ultimately increase the efficiency of that particular heat exchanger.

3.2 Modeling Damping Effect Caused by Microtextured Surface

Results from initial testing using the volume addition procedure would suggest that the microstructures of the surface actually play a significant role in the drop coalescence phenomena. Figure 3-2 shows the width vs. time plots of drops coalescing on substrates with 3.3μm, 50μm, and 100μm spacing. Each line represents the response from a representative sample experiment for each of the three micropost surfaces. The transient response of the water droplets during coalescence would indicate that the damping-like feature, or pinning, is associated with the interaction between the liquid and the solid at the interface.

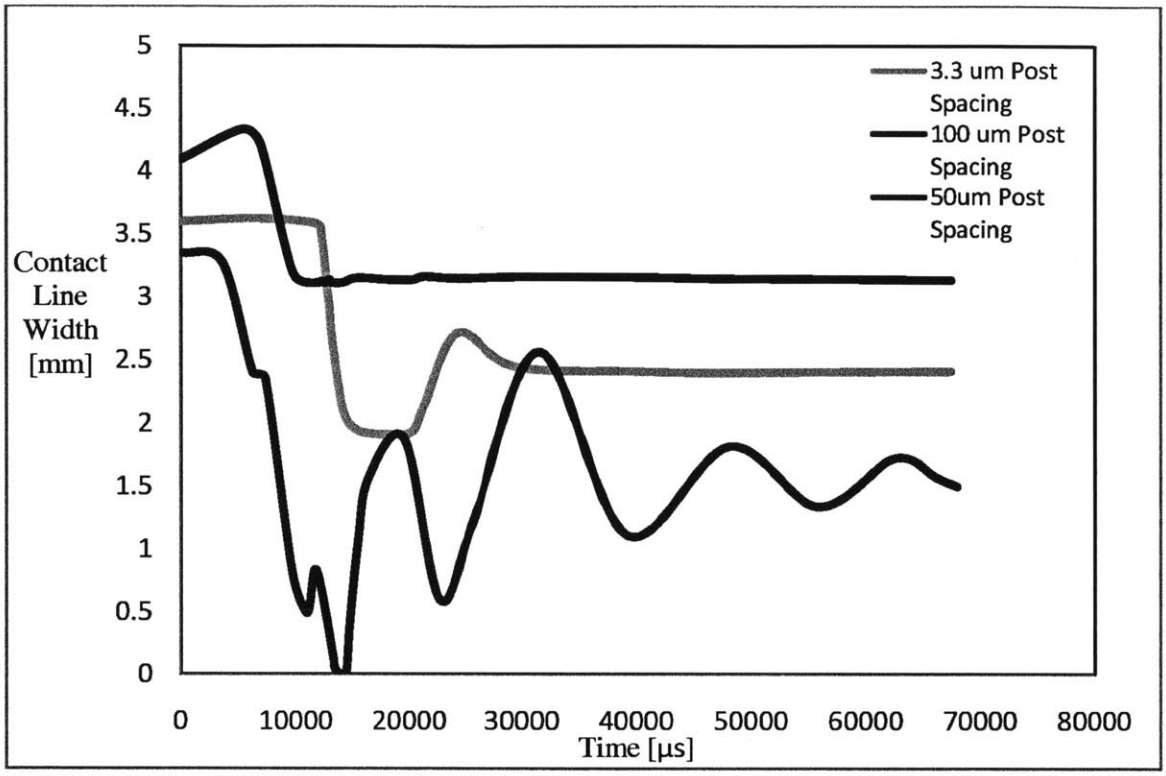

Figure 3-2: Contact Line Width vs. Time for Coalescence for representative sample experiments from 3.3, 50, and 100 μm post spacing.

The black curve is the transient response of the surface with 100μm post spacing. The response appears to be highly dampened, and reaches an equilibrium at roughly 12ms, much faster than the response on a more dense post spacing. The initial droplets, as shown in figure 3-3, were in the Wenzel state before coalescence was even initiated. During the process, waves propagated to opposite ends of the droplet and became pinned to the surface when retracting back to the center of the drop. The pinning at the ends of the droplet prevented the droplet from drastically changing width. Interestingly enough, the end width of the large drop is significantly higher than the width of the large drops on the other surfaces, almost twice as wide the equilibrium width for the substrate with 50μm post spacing. There seems to be a correlation between how strong the force is at the interface of the solid and the liquid and the final surface area covered by the droplet after coalescence.

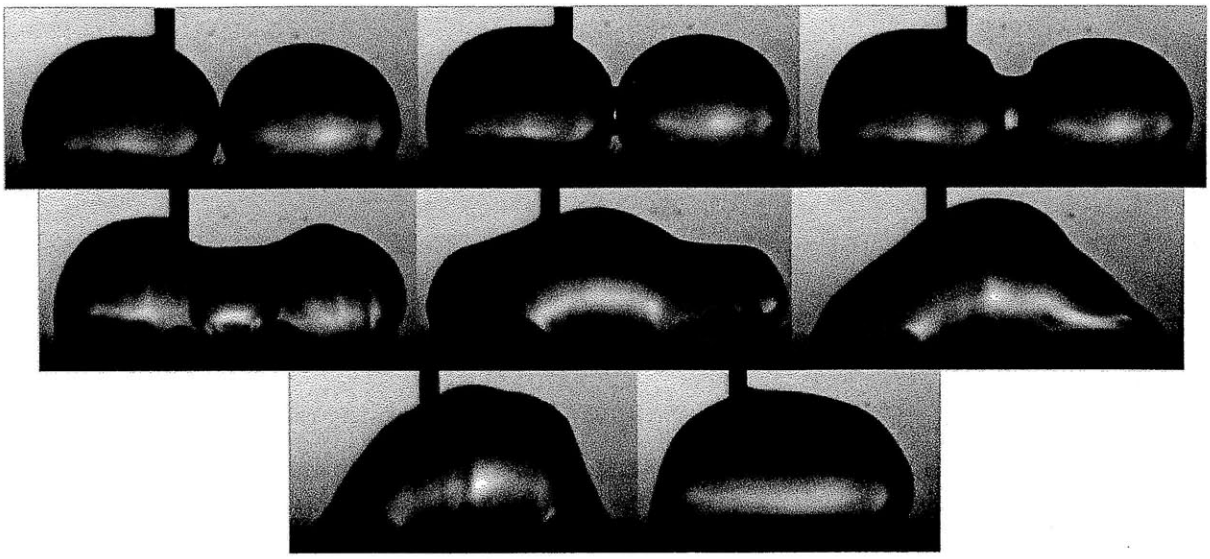

Figure 3-3: 100μm Post Spacing. From top left to bottom right, drop coalescence on the microtextured surface at t= -0.1, 0, 0.3, 1.3, 4.6, 6.7, 8.3, 16.7 ms

The light gray curve represents the surface with 3.3μm post spacing. The impact of the surface on the liquid in the 3.3μm experiment was much lower than that of the 100μm experiment. The drop exhibited slight oscillation about its equilibrium width, as shown in figure 3-4, but still dampened to its equilibrium shortly thereafter ($t \approx 35$ms). Of the substrates being characterized in this thesis, the sample with 100μm post spacing has the largest spacing between posts and the sample with 3.3μm post spacing has the smallest spacing between posts. Despite having the largest difference in post spacing, the impact they have on drop coalescence is far from having the greatest difference.

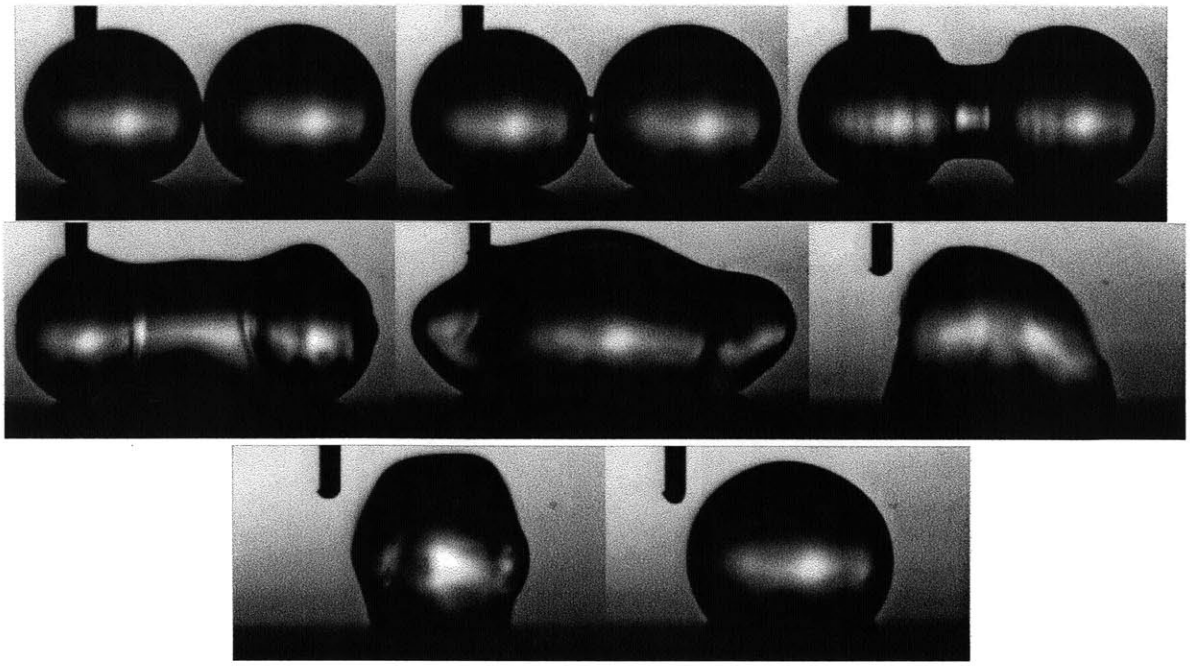

Figure 3-4: 3.3μm Post Spacing. From top left to bottom right, drop coalescence on the microtextured surface at t= -0.1, 0, 0.6, 2, 4.8, 6.9, 9.6, 76.6 ms.

The samples that exhibited the greatest difference in impact during coalescence were the samples with post densities near 50μm. The dark gray curve shows the response for the substrate with 50μm post spacing. Unlike the sample with 100μm post spacing, the sample with 50μm post spacing gave almost no resistance to drop movement during coalescence. The initial droplets, as shown in figure 3-5, were in the Cassie state. When the drops coalesced, they remained in Cassie state, barely wetting the surface throughout the process. Since so little of the water was being held to the surface during the process, the restitution of the water drop caused the droplet to actually lift up off of the surface and completely break contact with it for a short period of time. Upon landing back on the surface, the drop began oscillating towards its equilibrium state, still in the Cassie state. The lack of resistance allowed the drop to oscillate about its equilibrium point before eventually dampening to its equilibrium state in almost an order of magnitude longer than the time it took for the drop to reach equilibrium on the sample with 100μm post spacing ($t \approx 100$ ms).

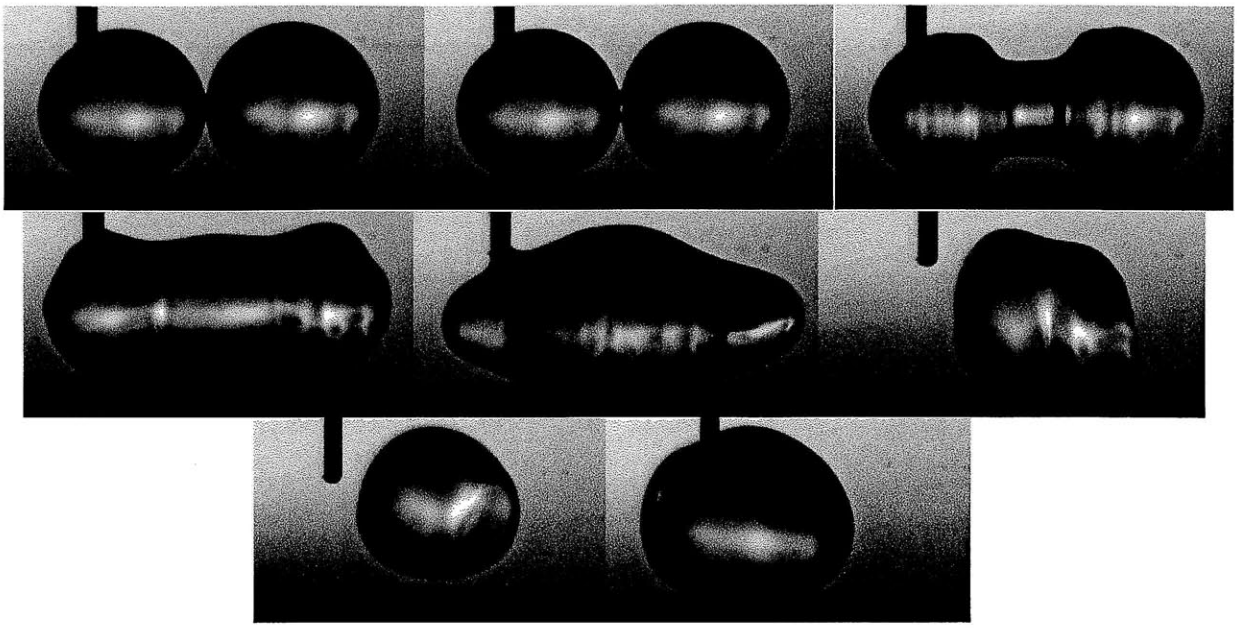

Figure 3-5: 50μm Post Spacing. From top left to bottom right, drop coalescence on the microtextured surface at t= -0.1, 0, 0.8, 2.2, 4.9, 7.3, 13.4, 58.2 ms.

In order to develop the physical model for the phenomenon on the microtextured surfaces, three main parameters will be observed. The total change in width from initiation of drop coalescence to its eventual relaxation on the surface will indicate the droplets tendency to wet on the surface. Small changes in width are indicative of greater wetting on the surface, whereas large changes in width are indicative of less wetting on the surface. The average settling time will also be examined in order to determine the physical model for drop coalescence on the microtextures surfaces. Longer relaxation times, as will be exhibited, suggest that the droplet is dampening at its own natural response. Fast relaxation times, on the contrary, would suggest that the interaction between the solid and the liquid at the three phase contact line is very strong and capable of relaxing the droplet much faster.

In order to characterize the damping effect on the droplet of water, the average contact line velocity will be examined. This parameter will essentially represent the slope of a decaying envelope following the transient response of the water droplet on the surface. A low contact line velocity would indicate that only a small amount of width has changed over a long period of time. For example, the 50μm post spacing experiment

shown in figure 3-2 has a very low contact line velocity when compared to the rapid contact line velocity of the 100μm post spacing experiment.

3.3 Droplet Behavior Resulting from Coalescence on Microposts

Contact Line Change in Width

From experimental observation, the wetting state of a droplet during coalescence greatly impacts the relaxation of the combined droplet immediately following initial contact of the two sessile water droplets. For the range of surfaces examined in this thesis, the total change in width from start to finish varied depending on the micropost spacing. Figure 3-6 shows the total change in width from initial contact to relaxation. At low and high post spacing, the drops exhibited very small changes in width from start to finish of the coalescence process. This was, in large part, due to the wetting state of the drops during coalescence. The sample with 100μm post spacing exhibited almost no net change in width. At the start of the process, the drops were already in the Wenzel state. The stability of the state increased the activation energy needed to move the drops. That energy did not appear during the coalescence process As shown in figure 3-3, the capillary waves were forced to the surface almost instantaneously and were dragged along the surface towards the bulk fluid. Since there was so much pinning at the three phase contact line, the droplet quickly reached contact angle equilibrium.

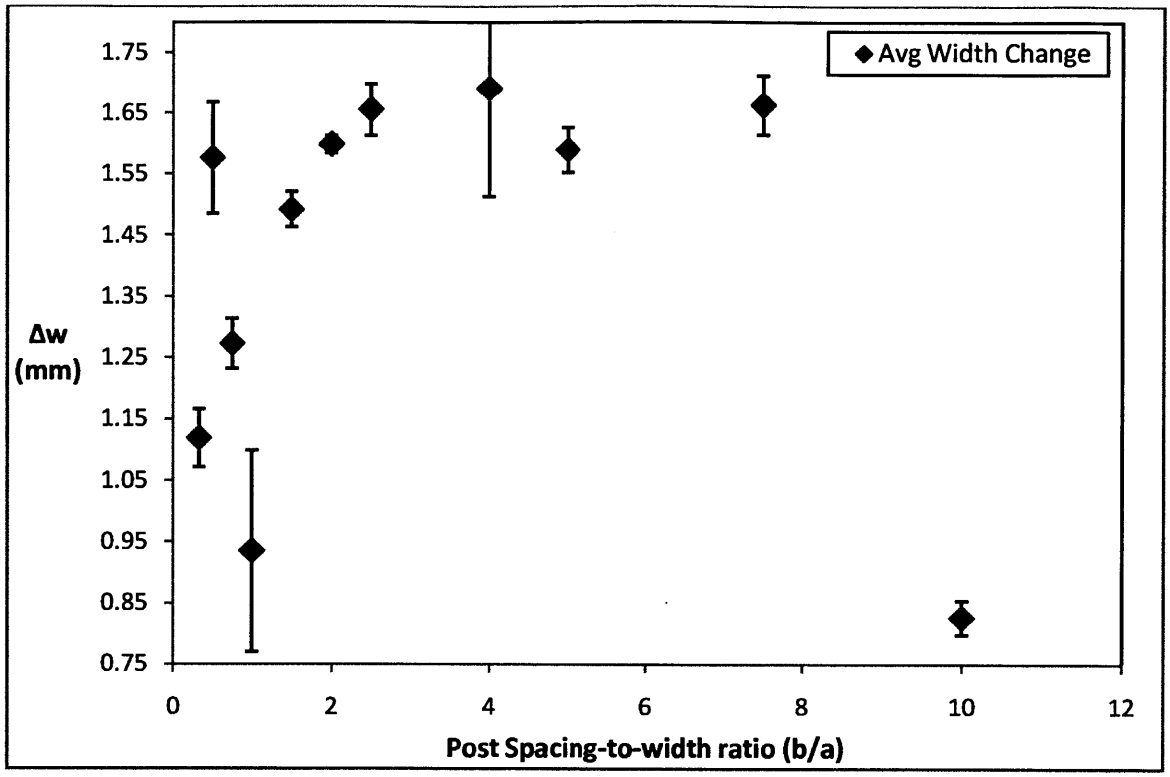

Figure 3-6: Total change in width vs. micropost spacing.

The samples that fell within the median range of post spacing experienced a significant change in width from start to finish. The large change experienced by the contact line was allowed to happen due to the droplets being in Cassie state throughout the entire process. The samples with relatively small post spacing were also in the Cassie state, but the droplets had already begun transitioning to the Wenzel state and remained somewhat pinned to the surface.

These results align well with current work being done in the Varanasi group. Surfaces with median range post spacing have been shown to exhibit very low hysteresis when compared to more dense or sparse post spacing. The ability for the droplets to move easily on the surface during drop coalescence correlates well with hysteresis data for roll off experimentation on those particular surfaces.

Contact Line Velocity

The trend of the contact line velocities is inverse of the trend shown in figure 3-6. The combination of having very little to travel and with significant force acting at its

three phase boundary, the sample with 100μm post spacing had the fastest contact angle velocity. Ideally, however, the contact angle velocity should be very slow. This is ideal because a slow contact angle velocity indicates that the drop oscillated for a significant amount of time before coming to a stop at the final equilibrium position. That being said, it is clear that the middle ranged post spacing samples exhibit that oscillation best.

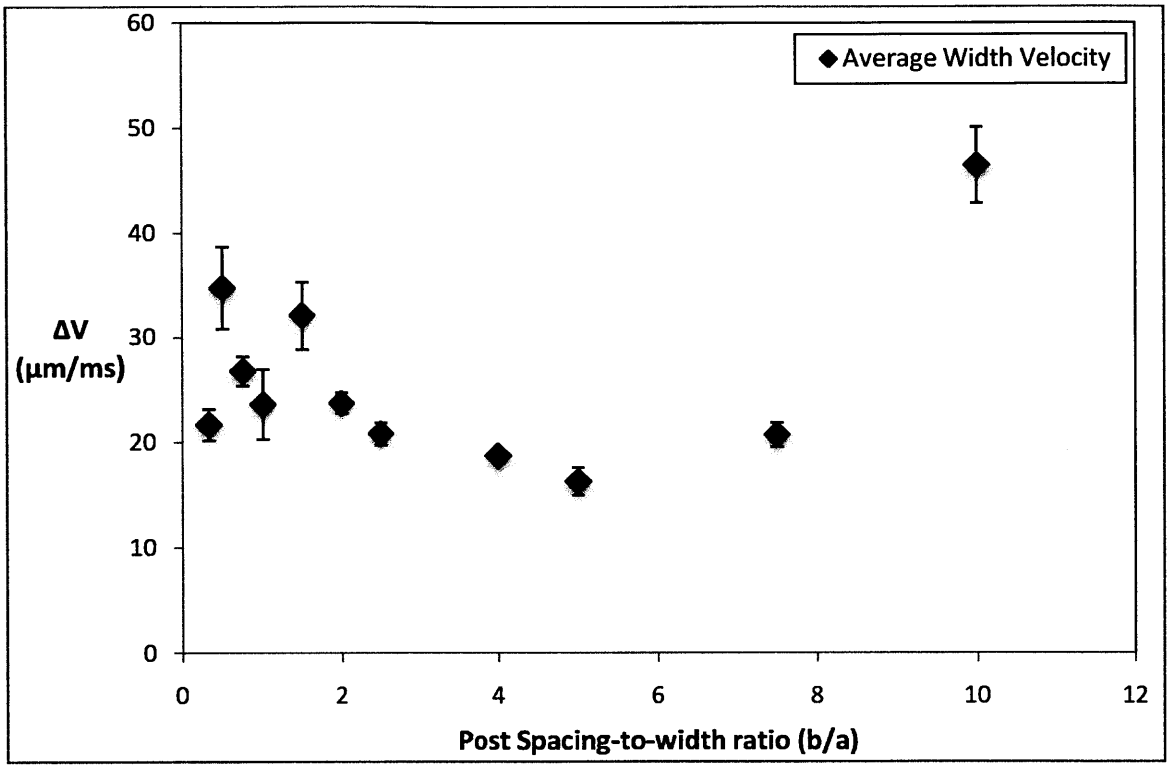

Figure 3-7: Contact line velocity vs. micropost spacing

Coalescence Relaxation Time

The relaxation time, shown for all samples in figure 3-8, is important information because it implies when the droplet reaches a stable position on the surface. For purposes of condensers, the relaxation time should be as long as possible because the drops would be more likely to just roll-off at any given point in time. If a stable position is reached, more net activation energy is required to move the droplet out of the way, which makes the system even more inefficient. Of the three data types, the 50μm post spacing sample outperformed all the other samples because it would allow for easy removal of drops for

a surface and keep the drops at an instable equilibrium until a large enough force could move it out of the way. The trend seems to show that rather than a direct correlation to post spacing, there is actually an optimal balance in the spacing of the posts to obtain a desired coalescence behavior.

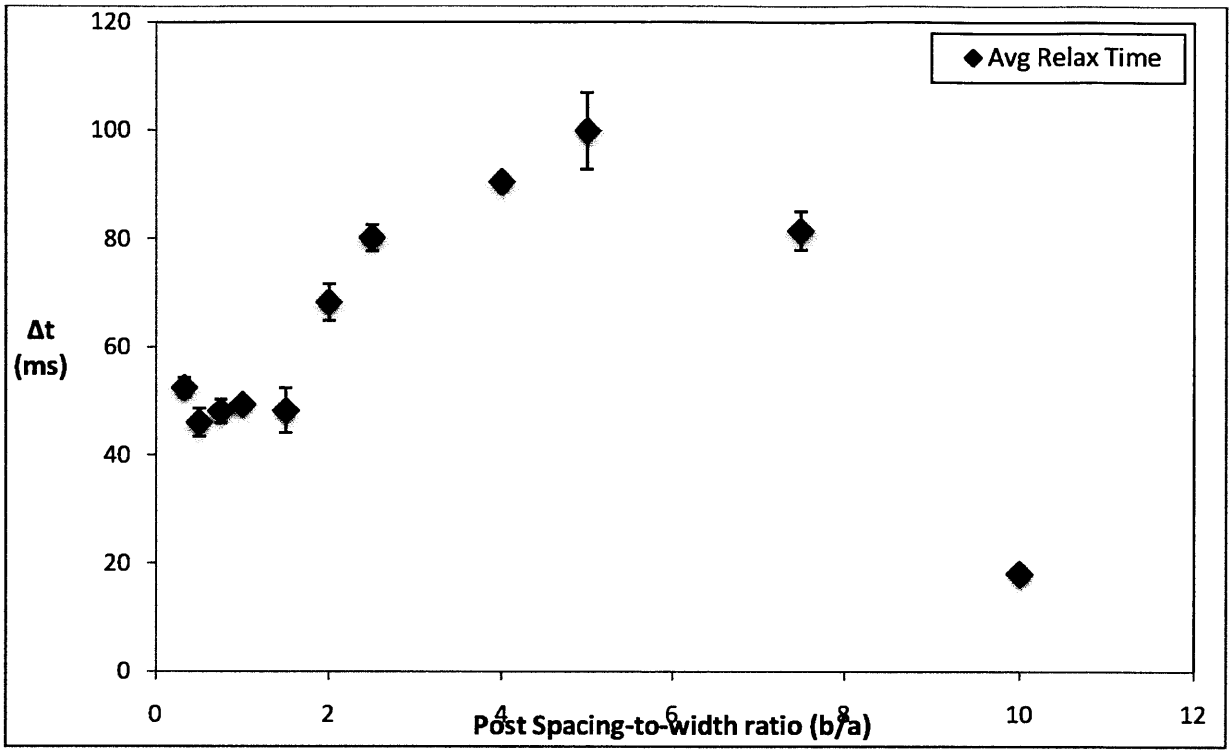

Figure Y: Relaxation time of droplet vs. Micropost spacing

3.4 Capillary Wave Propagation After Liquid Bridge Formation

After initial contact and well into the inertial regime, the capillary waves that propagate outward from the contact of the two drops continue until the viscosity of the fluid retracts the fluid towards its center. Interestingly enough, the state of the sessile drop on the surface played a large role in the dynamics of the capillary waves. During a volume addition experiment on the surface with 50μm post spacing, one of the drops transitioned to Wenzel state, while the other remained in the Cassie state. Drop coalescence was initiated and the capillary waves initially propagated as expected, but changed when the

capillary wave on the Wenzel drop reached the surface, shown in figure 3-6. At that point, the wave stopped, reversed direction and began completely wetting the surface towards the drop that was in the Cassie state. The reversed wave pulled the Cassie drop towards the already wet region and the combined droplet instantly was in the Wenzel state where the movement of the droplet dampened rapidly, settling to its final width at $t \approx 20ms$. This experiment further shows the dominance of a Wenzel droplet compared to a Cassie droplet. For this thesis, the desired micropost structure for drop-wise condensation on a surface would allow a drop to remain in Cassie state throughout the entire process of drop coalescence.

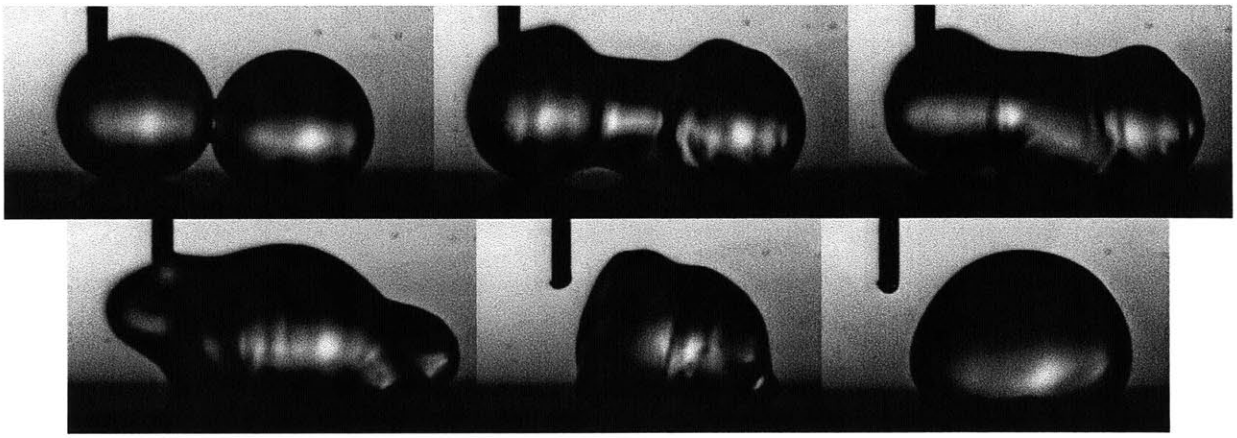

Figure 3-6: Wenzel drop coalescing with Cassie Drop.

4 Physical Model for Microstructured Surface Effects on Drop Coalescence After Drop Impact

4.1 Modeling Receding Break Up Drop Impact Scenario

As previously mentioned, there are many scenarios that can describe a particular situation for drop impact. For this thesis, the receding break up scenario is desired for the purpose of inducing coalescence between two drops at collision. Other scenarios would not be ideal due to the difficulty involved with coordinating the drops with enough accuracy to view the process consistently. In order to assure that the receding break up scenario occurs, the height of the stand was set high enough that the drop would gain enough velocity to yield a high Reynolds number.

A micropost surface was used to release the droplets from the droplet device due to its high hydrophobicity. Initial testing resulted in consistent surface and drop collision for experimental observation. Figure 4-1 shows the progression of two droplets colliding with the surface then with each other as well as the retraction that occurs after all the kinetic energy has been dissipated.

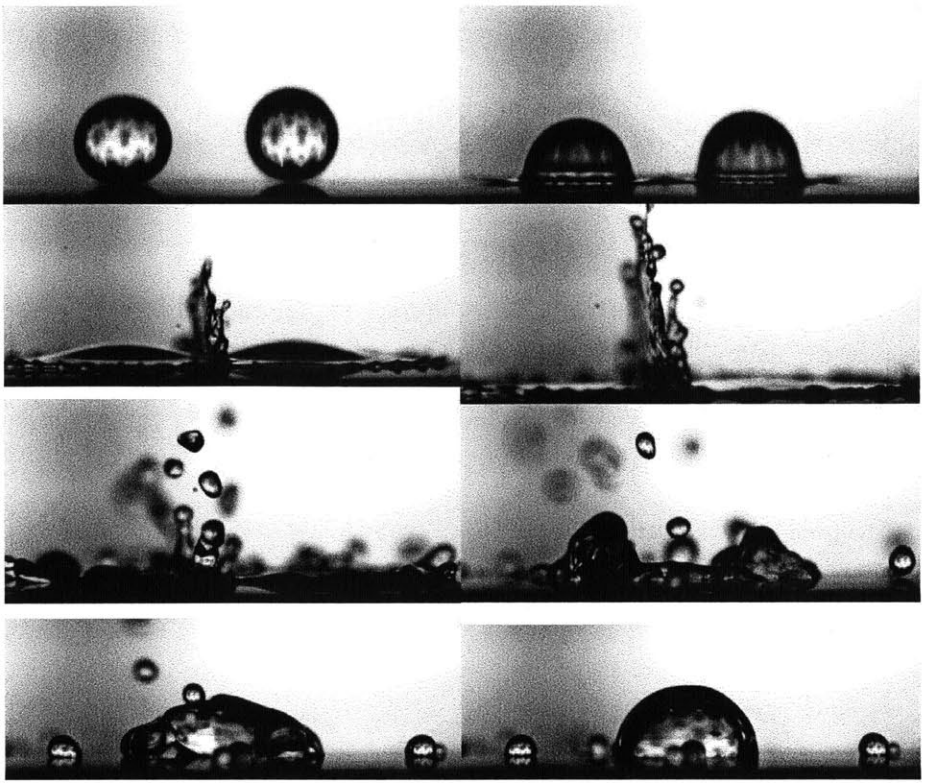

Figure 4-1: 100μm Post Spacing for Drop Impact Experimentation

The droplets, upon colliding with the surface, began to spread out as expected. Shortly after colliding with the surface ($\approx$ 2.8 ms), the drops dissipated most of their kinetic energy and fingers began to pinch off from the ends of the film created by the water. Satellite drops resulted from that disconnect and a bulk of the water was able to retract back to one large drop. The coalescence of the fluid upon impact relied heavily on the distance between the two drops on impact.

4.2 Experimental Observation of Variance Across Different Microtextures

Upon examining the coalescence during drop impact, a correlation similar to the volume addition experimenatation was apparent. At very sparse and very dense post spacing, the drops were able to retract back to one bulk droplet after only having lost a few satellite drops. However, the mid-range post spacing left two medium sized drops sitting right next to each other. One explanation for the phenomena would be the surface

tension at the dynamic contact line. At sparse post spacing, there seems to be a high surface tension at the three phase contact line. The kinetic energy of the droplet, rather than continuing outward and overpowering the viscous forces in the fluid, gets dissipated by the surface tension upon contact. This dissipation keeps the fluid relatively close together.

One direct correlation that was observed was the height of the wave caused by the two drops clashing after impact. Figure 4-2 shows the difference in wave height according to post spacing of the surface. More densely spaced posts yielded less energy for the colliding liquid to propel upward. Less satellite drops broke off from the more densely spaced post surfaces from the colliding wave.

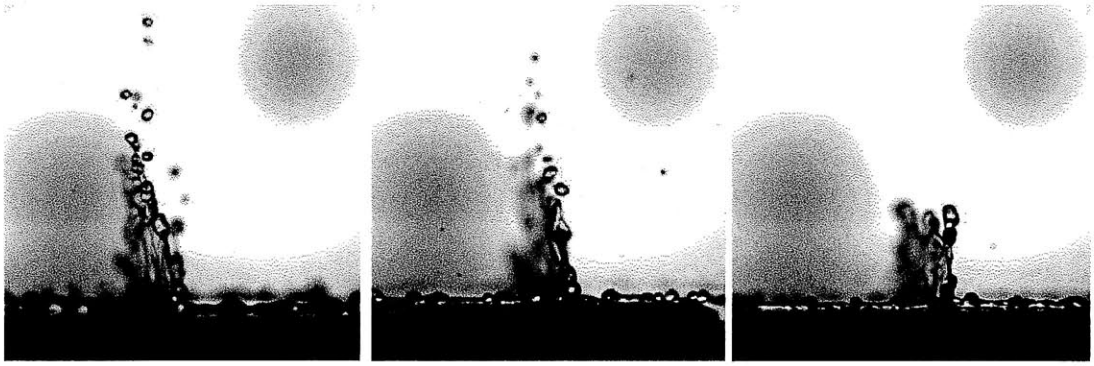

100μm - 12mm 50μm - 10mm 15μm - 4.68mm

Figure 4-2: Waves caused by clashing drops immediately after impact. Each image shows the maximum wave height before satellite drops break free. The numbers below the images represent the post spacing (left) and maximum height (right).

5 Conclusions and Recommendations

This thesis has explored the phenomena of drop coalescence on microtextured surfaces and provided a fundamental physical understanding of how surface wetting and surface tension at the three phase contact line can significantly affect the resulting response of drop coalescence. This fundamental understanding can offer a solid foundation for future work in surface design to control drop coalescence on its surface. This thesis concluded that there exists an optimum aspect ratio for micropost surfaces that controls how a droplet wets on a surface during drop coalescence. Drop coalescence on surfaces with aspect ratios that are smaller or larger than the optimum ratio are very likely to end up in a stable Wenzel state, ideal for film-wise condensation. Industrially, being outside of that threshold is not beneficial for heat transfer in a condenser. Having a surface that behaves within the aforementioned optimum aspect ratio will yield drop-wise coalescence at the surface that is unstable and easily removed from the surface, a desired property in nano-engineered surfaces known as self-cleaning. Relaxation times were also experimentally shown for a range of micropost surfaces and as a result yielded contact line velocities that further helped develop the physical model for the phenomenon that occurs on these microtextured surfaces.

Wetting was shown to have significant impact on both volume addition and drop impact studies in this thesis. The change in activation energy needed to move a droplet after it has transitioned to the Wenzel state is far too great for viscous forces to overcome. The ability to control they hysteresis of the water droplet will be a key factor in the eventual control of drop coalescence on nano-engineered surfaces.

Preliminary experimentation has shown promise for future work in drop impact testing pertaining to drop coalescence and wetting. The development of a more consistent experimental set up would allow for more reliable data along the spectrum of surfaces being tested. Quantitative data would also help in further developing a model to describe drop coalescence after drop impact on a nano-engineered surface. Had more time been available, testing across a greater combination of surfaces would have helped in better developing a physical model for the drop impact coalescence.

6 Appendix A: Detailed Procedures for Experimentation

6.1 Volume Addition Procedure

After the first drop is placed on the surface, prepare the software to capture the desired data as well as save it after the experiment is complete. Set the imaging rate to 10000fps at the highest resolution possible for that frame rate. Also set the trigger mode to "end" so as to capture the event after it has already occurred. To save the data, indicate a save path for the file as well as the desired format of the video.

After all things are set in place, raise the needle and slide the substrate a set amount depending on how the droplet sits on the surface. In order to determine how far to slide the substrate the radius of the droplet on the surface must be known. The radius is pertinent because it is the parameter that will indicate how far the next drop has to be placed in order for the two to coalesce at known volumes. If the drops are too far apart, coalescence never occurs, but if the two are too close to each other, then coalescence happens between a droplet with a known volume and a droplet with an unknown volume.

After sliding the substrate over by the distance needed between the two droplets, lower the needle and prepare to add a droplet to the surface. The second drop is much more crucial in the process because it is the effecter of the system. The drop must be very still when approaching the other droplet as to avoid adding unwanted energy into the system such as oscillations on the drop surface. Using the drop deposition software, assign a deposition value at a slow stroke time and initiate image capture on the high speed video camera. Once coalescence occurs, select capture on the high speed video software to save the two seconds leading up to when capture was selected. The video will appear on the screen and can be cut down to save only the desired images. Save the video and proceed to the next experiment. The steps for the experimentation are as follows:

1. Deposit 6 μL at 500s stroke time
2. Raise the needle and slide the substrate over a desired amount
3. Lower needle and deposit 3 μL at 500s stroke time
4. Begin recording on Photron Fastcam Viewer software
5. Deposit 3 μL at 1200s stroke time
6. Immediately after coalescence occurs, end video capture to record the event
7. Save data in desired folder and in desired format
8. Clean substrate for more experimentation

6.2 Drop Impact Procedure

The experimental set up is almost identical to the set up for volume addition, but instead of a needle attached to a volume addition device, a droplet device is attached to a laboratory stand at a desired distance from the surface. Using a precision pipette, DI water should be added gently to the surface of the droplet device as to avoid allowing the water to transition into Wenzel state. In the event that a drop does transition into Wenzel prior to being dropped onto the surface, the drop needs to be removed and the experiment restarted. Outlined below is the procedure for the drop impact experimentation:

1. Add desired amount of DI water to surface of droplet device. Make sure that the volume is lower than 8μL to ensure that the drop stays spherical as it falls toward the surface.
2. Adjust the camera to focus on an object that is in the same position as the drops will be as they fall during experimentation.
3. Initiate camera software to begin capturing video for impact testing.
4. Remain near the computer to terminate video after the drops impact the surface.
5. Add the second drop of water next to the first drop at the distance of interest.
6. Pull the latch that will release the droplet plank to allow the drops to fall to the surface.
7. Immediately terminate the video capture upon impact of the droplets.

8. Clean the surface of the droplet device as well as the impact surface for further experimentation.

7 Appendix B: Detailed Design of Droplet Device

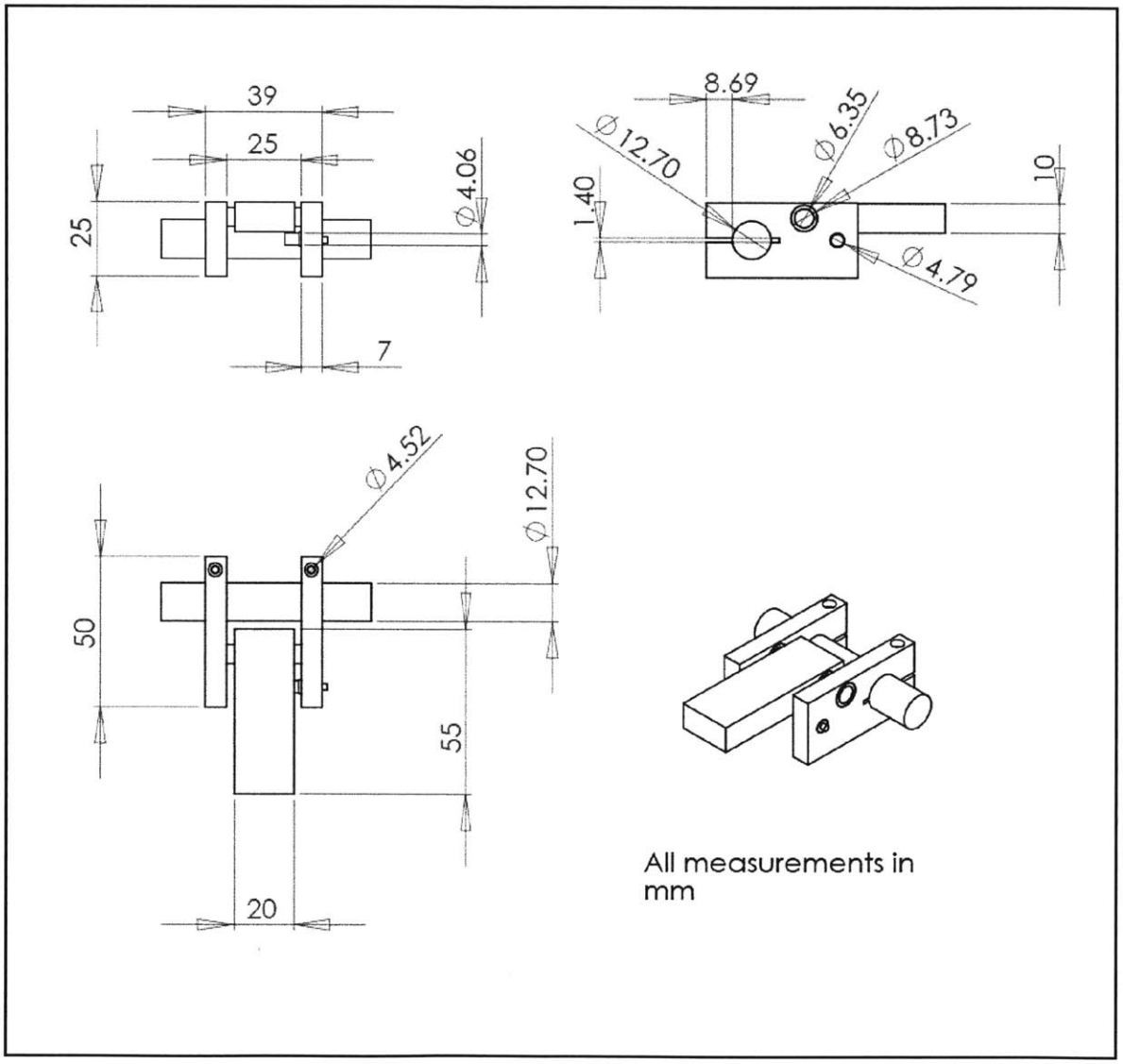

Bibliography

1. Narhe, R., Beysens, D. & Nikolayev, V.S. Contact Line Dynamics in Drop Coalescence and Spreading. *Langmuir* **20**, 1213-1221 (2004).
2. Eggers, J., Lister, J.R. & Stone, H.A. Coalescence of Liquid Drops. *Journal of Fluid Mechanics* **401**, 293-310 (1999).
3. Aarts, D.G.A.L., Lekkerkerker, H.N.W., Guo, H., Wegdam, G.H. & Bonn, D. Hydrodynamics of Droplet Coalescence. *Phys. Rev. Lett.* **95**, 164503 (2005).
4. Paulsen, J.D., Burton, J.C. & Nagel, S.R. Viscous to Inertial Crossover in Liquid Drop Coalescence. *Phys. Rev. Lett.* **106**, 114501 (2011).
5. Wu, M., Cubaud, T. & Ho, C.-M. Scaling law in liquid drop coalescence driven by surface tension. *Phys. Fluids* **16**, L51 (2004).
6. Blanchette, F. & Bigioni, T.P. Partial coalescence of drops at liquid interfaces. *Nat Phys* **2**, 254-257 (2006).
7. Yokota, M. & Okumura, K. Dimensional crossover in the coalescence dynamics of viscous drops confined in between two plates. *Proceedings of the National Academy of Sciences* (2011).doi:10.1073/pnas.1017112108
8. Case, S.C. & Nagel, S.R. Coalescence in Low-Viscosity Liquids. *Phys. Rev. Lett.* **100**, 084503 (2008).
9. Aryafar, H., Lukyanets, A.S. & Kavehpour, H.P. Inertia-Dominated Coalescence of Drops. *Applied Mathematics Research eXpress* **2006**, (2006).
10. Quéré, D. Non-sticking drops. *Rep. Prog. Phys.* **68**, 2495-2532 (2005).
11. Wenzel, R.N. Resistance Of Solid Surfaces To Wetting By Water. *Industrial & Engineering Chemistry* **28**, 988-994 (1936).
12. A. B. D. Cassie, "Contact angles," *Discussions of the Faraday Society* 3 (1948): 11-16.
13. Eggers, J., Fontelos, M.A., Josserand, C. & Zaleski, S. Drop dynamics after impact on a solid wall: Theory and simulations. *Phys. Fluids* **22**, 062101 (2010).
14. Thoroddsen, S.T. & Takehara, K. The coalescence cascade of a drop. *Phys. Fluids* **12**, 1265 (2000).
15. Neinhuis, C. & Barthlott, W. Characterization and Distribution of Water-repellent, Self-cleaning Plant Surfaces. *Annals of Botany* **79**, 667 -677 (1997).
16. Kripa K. Varanasi et al., "Design of Superhydrophobic Surfaces for Optimum Roll-Off and Droplet Impact Resistance," *ASME International Mechanical Engineering Congress and Exposition* (October 31-November 6, 2008): IMECE2008-67808.
17. Yarin, A.L. Drop Impact Dynamics: Splashing, Spreading, Receding, Bouncing.... *Annu. Rev. Fluid Mech.* **38**, 159-192 (2006).
18. Mundo, C., Sommerfeld, M. & Tropea, C. Droplet-wall collisions: Experimental studies of the deformation and breakup process. *International Journal of Multiphase Flow* **21**, 151-173 (1995).
19. Gao, L. & McCarthy, T.J. Contact Angle Hysteresis Explained. *Langmuir* **22**, 6234-6237 (2006).